Structure of a DNA−Bisdaunomycin Complex[†,‡]

Gary G. Hu,[§] Xiuqi Shui,[§] Fenfei Leng,[∥] Waldemar Priebe,[⊥] Jonathan B. Chaires,[∥] and Loren Dean Williams*[,§]

School of Chemistry & Biochemistry, Georgia Institute of Technology, Atlanta, Georgia 30332-0400, Department of Biochemistry, University of Mississippi Medical Center, Jackson, Mississippi 39216-4505, and University of Texas M. D. Anderson Cancer Center, Houston, Texas 77030

Received March 6, 1997; Revised Manuscript Received April 3, 1997[⊗]

ABSTRACT: The application of detailed structural data bases has now culminated in the successful design of a new generation of bisanthracyclines that form ultratight DNA complexes [Chaires, J. B., Leng, F., Przewloka, T., Fokt, I., Ling, Y. H., Perez-Soler, R., & Priebe, W. (1997) *J. Med. Chem. 40*, 261−266]. Daunomycin dimers were designed to bind to DNA in complexes resembling those of monomers intercalated at adjacent sites. The goal of the work described here was to determine, with X-ray crystallography, if a potent member of this newly designed and synthesized class of bisanthracyclines (WP631) binds as intended. WP631 is composed of two daunomycin molecules, linked N3′ to N3′ by a xylyl group. We have solved the 2.2 Å X-ray crystal structure of a complex of WP631 bound to $[d(CGATCG)]_2$. We demonstrate, on a detailed molecular level, that the WP631 design strategy is a success. The structures of WP631 and two daunomycin molecules bound to $[d(CGATCG)]_2$ provide the unprecedented opportunity for detailed comparison of mono- and bis-intercalated complexes of the same chromophore, allowing us to distinguish effects of mono-intercalation from those of bis-intercalation. Differences are focused primarily in the centers of the complexes. DNA unwinding and other helical distortions propagate more efficiently to the center of the WP631 complex than to the center of the daunomycin complex.

Anthracyclines such as daunomycin and adriamycin rank among the most potent and clinically useful treatments for certain widespread cancers (Boulad & Kernan, 1993). Because of daunomycin, for example, acute myeloid leukemia is no longer a uniformly fatal disease. The direct relationship between anthracycline activity and DNA affinity (Valentini et al., 1985) has provoked interest in the chemical conversion of mono-intercalative anthracyclines to bis-intercalative forms. Ideally, the binding constant of a bis-intercalator is the square of that of the monomer. Appropriate coupling of a mono-intercalative anthracyclines into bis-intercalators could dramatically increase DNA affinity and, therefore, activity.

Modification of parent anthracyclines, daunomycin and adriamycin, has failed to yield dramatically improved clinical agents. These failures arose in part from the lack of incorporation of structural and other physical−chemical data into design processes. A foundation is now laid for a structure-based pipeline for bis-anthracyclines. This foundation, accumulated over several decades by many investigators, is comprised of detailed structural, thermodynamic and kinetic data. The nucleic acid data base contains three-dimensional structures of over 20 DNA−anthracycline complexes. The thermodynamics (Chaires et al., 1996; Remeta et al., 1991) and kinetics (Chaires et al., 1985; Krishnamoorthy et al., 1986; Rizzo et al., 1989) of anthracycline−DNA interactions are similarly well-characterized.

It appears that the application of these data bases has culminated in the successful design of a new generation of bis-anthracyclines (Chaires et al., 1997). The design goal was a daunomycin dimer that would bind to DNA in a complex resembling that of the intercalated monomers. The three-dimensional X-ray structure of a DNA complex of two daunomycin monomers was used as a template to build linkers giving appropriate proximity and orientation of dimerized chromophores. This incorporation of three-dimensional ligand−macromolecular information is a departure from earlier, essentially unsuccessful efforts at bis-anthracycline design.

A potent member of this newly designed and synthesized class of bisanthracyclines is WP631 (Figure 1). Solution studies confirm that, as intended, WP631 bis-intercalates in DNA with high affinity (Chaires et al., 1997). Preliminary cytotoxicity studies indicate promising clinical potential. Currently, the effectiveness of anthracyclines is considerably compromised by multidrug resistance (MDR). MDR is caused by increased drug efflux after induction of P-glycoprotein (Ross, 1991). Circumvention of resistance is thought to be necessary for further enhancement of cure rates. WP631 overcomes MDR in human carcinoma cell lines, showing greater cytotoxicity against MDR lines than against sensitive cells (Chaires et al., 1997).

The goal of the work described here was to determine, with X-ray crystallography, if WP631 binds to DNA as designed. We determined the structure of WP631 bound to $[d(CGATCG)]_2$ and demonstrate, on a detailed molecular level, that the WP631 design strategy is a success. The results provide the unprecedented opportunity for detailed comparison of mono- and bis-intercalated complexes of the

[†] This work was supported by the National Cancer Institute (Grant CA35635 to J.B.C.), the National Science Foundation (Grant MCB-9056300 to L.D.W.), and the American Cancer Society (Grant NP-912 to L.D.W.).

[‡] The atomic coordinates have been deposited with the Brookhaven Protein Data Bank (entry 1AGL).

* Author to whom correspondence should be addressed.

[§] Georgia Institute of Technology.

[∥] University of Mississippi Medical Center.

[⊥] University of Texas M. D. Anderson Cancer Center.

[⊗] Abstract published in *Advance ACS Abstracts,* May 1, 1997.

S0006-2960(97)00521-7 CCC: $14.00

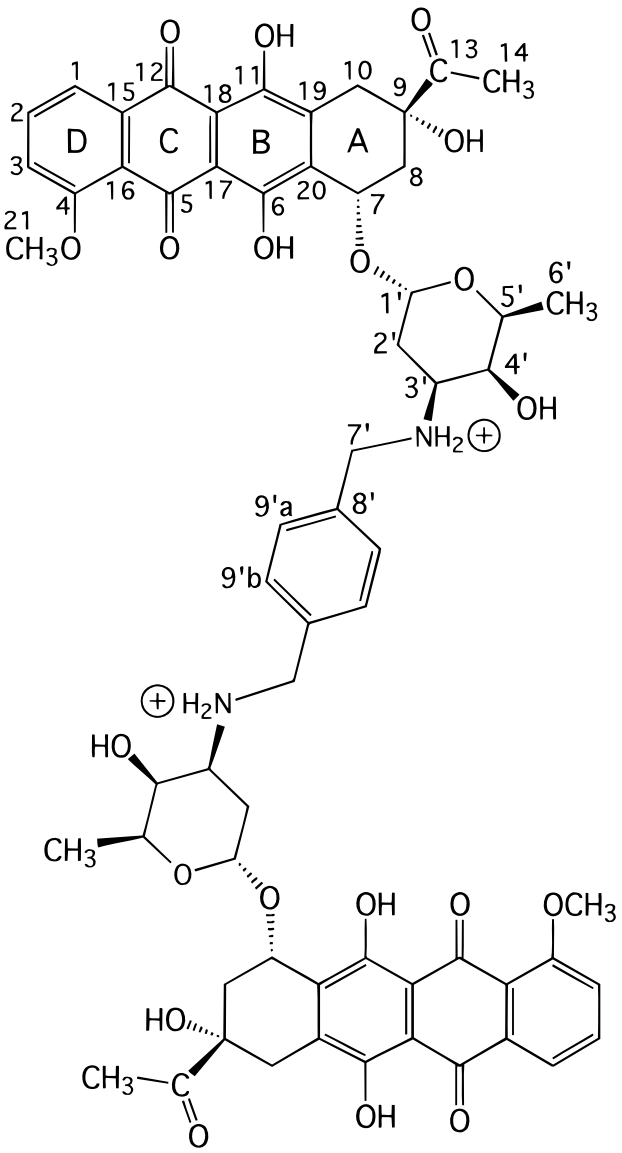

FIGURE 1: Chemical structure of WP631.

same chromophore. A comparison of DNA complexes of daunomycin and WP631 allows us to distinguish effects of mono-intercalation from effects of bis-intercalation. In addition, our results suggest that the design of WP631 might be refined to increase DNA affinity even further.

EXPERIMENTAL PROCEDURES

Crystallization. The ammonium salt of reverse-phase HPLC-purified d(CGATCG) was purchased from the Midland Certified Reagent Co. (Midland, TX). WP631 was synthesized as described (Chaires et al., 1997). Crystals were grown from sitting drops that initially contained 0.9 mM d(CGATCG), 36 mM sodium cacodylate (pH 6.5), 2.8 mM $MgCl_2$, 5% 2-methyl-2,4-pentanediol (MPD), 5.7 mM spermine tetrahydrochloride, and 0.5 mM WP631. The drops were equilibrated by vapor diffusion against a reservoir containing 30% MPD. Tetragonal ($P4_12_12$) crystals appeared within 3 months and grew to sizes of 0.2 × 0.3 × 0.2 mm.

Data Collection and Refinement. X-ray intensity data were collected at room temperature with San Diego Multiwire Systems (ADSC) area detectors. Copper Kα radiation (λ = 1.5418 Å) was generated with a fine-focus Rigaku RU200 rotating anode. Data were merged and reduced with ADSC software. Excluding solvent molecules, the coordinates of daunomycin bound to d(CGATCG) (Lipscomb et al., 1994) were used as a starting model for the refinement. The structure was annealed and refined, and sum ($2F_o - F_c$) and difference ($F_o - F_c$) Fourier maps were calculated with XPLOR (version 3.1; Brunger et al., 1987).

The internal crystallographic 2-fold axis that passes through the center of the xylyl group of the WP631 presented special difficulties during the refinement. To properly restrain planarity of atoms related by the 2-fold symmetry, the refinement was performed at lower symmetry and the 2-fold symmetry was imposed by averaging after each cycle of refinement. Models and maps were displayed on Silicon Graphics Indigo workstations. The linker of WP631 was docked into Fourier maps, and its position was manually readjusted with the program CHAIN (Sack, 1990) several times during the course of the refinement. In the final maps, the electron density is clean and continuous around both the DNA and the bis-intercalator (Figure 2). The position and interactions of the linker are unambiguous. Data collection and refinement statistics are presented in Table 1.

Table 1: Crystallographic Parameters

Data Collection and Refinement Statistics			
unit cell dimensions	a = 28.27 Å	b = 28.27 Å	c = 53.77 Å
	α = 90.0°	β = 90.0°	γ = 90.0°
space group			$P4_12_12$
temperature (°C)			21
number of collected reflections to 2.2 Å			11 192
number of unique reflections to 2.2 Å			1324
number of reflections used for refinement [$>3\,F/\sigma(F)$]			1061
R-merge (%)[a]			6.96
R-factor (%)			19.9
R-free (%)			31.4
rms deviation of bonds from ideality (Å)			0.014
rms deviation of angles from ideality (deg)			3.1
number of observed solvent molecules H_2O			8
overdeterminacy ratio			1.6

Number of Reflections, R-factor, and Completeness by Resolution

resolution range (Å)	no. of reflections	R-factor (%)	completeness[b] (%)
4.34−12.00	155	18.8	85.2
3.47−4.34	146	18.4	87.0
3.04−3.47	137	14.1	86.6
2.77−3.04	136	23.4	86.4
2.57−2.77	139	22.5	87.2
2.42−2.57	119	22.2	85.6
2.30−2.42	118	23.9	84.4
2.20−2.30	111	28.5	82.8

[a] R-merge = sum[abs(ave−obs)]/sum(ave). [b] After sequestering 10% for R-free.

RESULTS

WP631 bis-intercalates in the hexamer duplex (Figure 3). We denote the DNA residues of each complex as 5′-C(1)G-(2)A(3)T(4)C(5)G(6)-3′ for the first strand and 5′-C(7)G-(8)A(9)T(10)C(11)G(12)-3′ for the second strand. Base pairs are C(1)-G(12), G(2)-C(11), and so on. WP631 intercalates between base pairs C(1)-G(12) and G(2)-C(11) and between base pairs C(5)-G(8) and G(6)-C(7). The asymmetric unit consists of a single strand of DNA and half of a WP631 molecule. A crystallographic 2-fold rotation axis passes through the center of the benzyl ring of the linker and between the A(3)-T(10) and T(4)-A(9) base pairs.

The effects of conversion from mono-intercalation to bis-intercalation on DNA conformation are most pronounced in

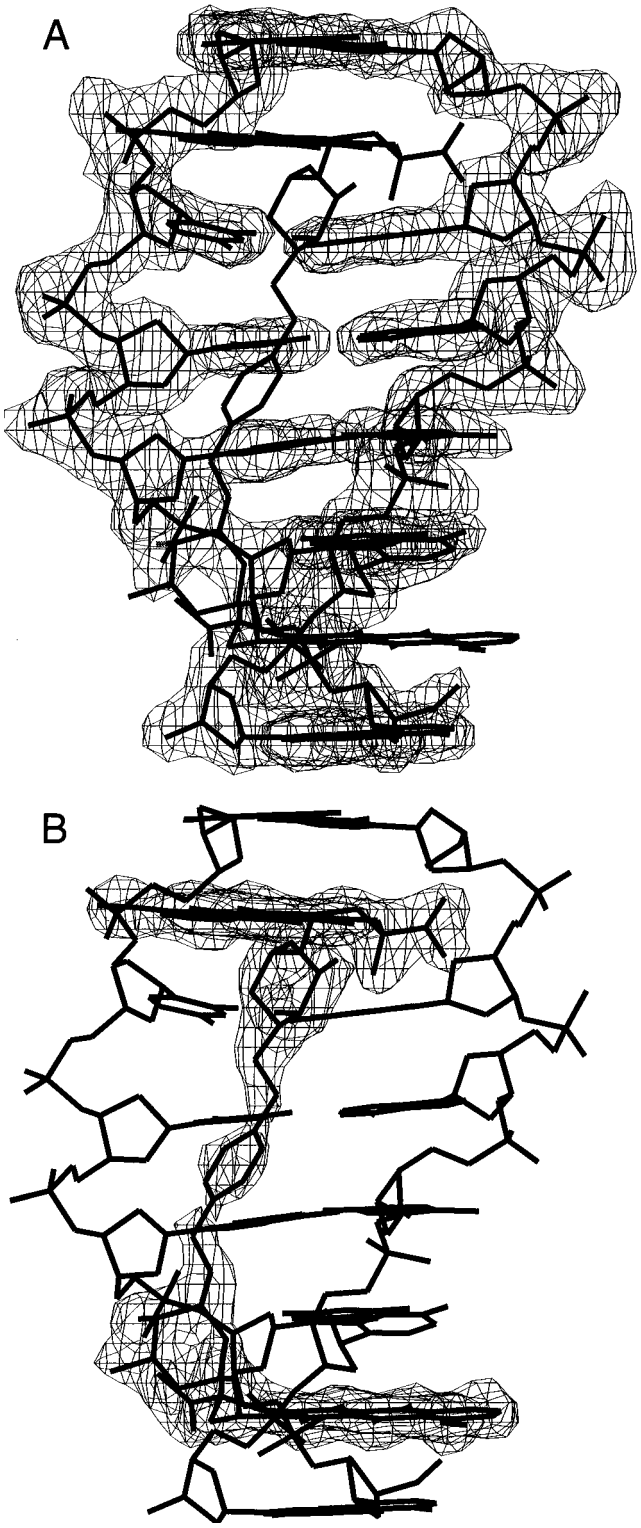

FIGURE 2: Sum ($2F_o - F_c$) electron density map surrounding (A) the DNA and (B) WP631.

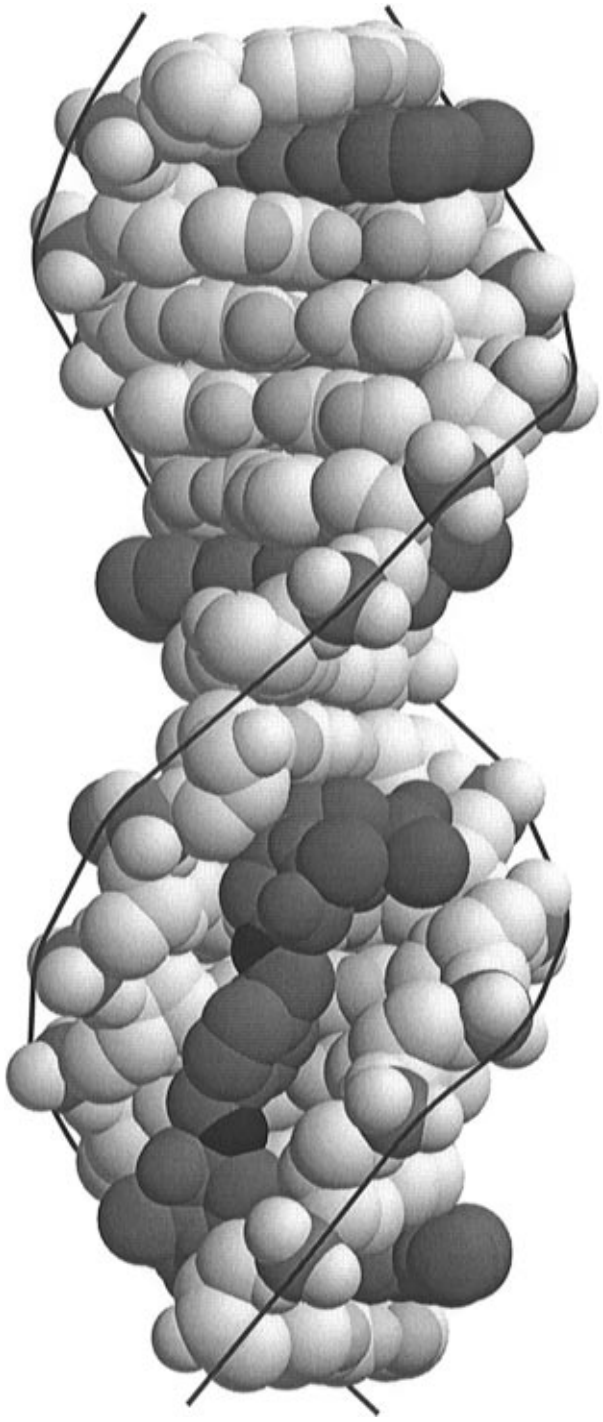

FIGURE 3: Space-filling representation of two WP631−[d(CGATCG)]$_2$ complexes as they are stacked in the crystal, approximating an infinitely long DNA duplex. The top of the figure shows a view into the major groove. The bottom shows a view into the minor groove. The two WP631 molecules are darker than the DNA. The N3′ nitrogen atoms of WP631 are black. Phosphorus atoms of the DNA are darkened. For clarity, lines trace the DNA phosphodiester backbones, passing over the missing phosphates at the seam between complexes in the crystal.

the center of the complex. A comparison of helical parameters of the WP631 and daunomycin complexes reveals that the DNA conformation is most conserved at the intercalation sites [i.e., at the C(1)−G(2) and C(5)−G(6) steps] and most disparate in the centers of the complexes. A superimposition of the WP631 and daunomycin complexes is shown in Figure 4, and differences in helical parameters are given in Table 2. Neither the mono- nor the bis-intercalated complex unwinds DNA at the site of intercalation [$\Delta\text{twist}_{\text{step }1-2} = -1.1°$; Δ values are those observed in the daunomycin complex (Lipscomb et al., 1994) subtracted from those observed in the WP631 complex]. Significant differences in DNA unwinding are observed in centers of complexes ($\Delta\text{twist}_{\text{step }2-3} = 6.8°$, $\Delta\text{twist}_{\text{step }3-4} = -5.3°$). The greatest differences in interbase shift and slide are for the G(2)−A(3) step ($\Delta\text{shift}_{2-3} = 1.0$ Å, $\Delta\text{slide}_{2-3} = 1.5$ Å). These parameters reflect differences in the position of A(3). G(2) is the most conserved residue in the complex. The

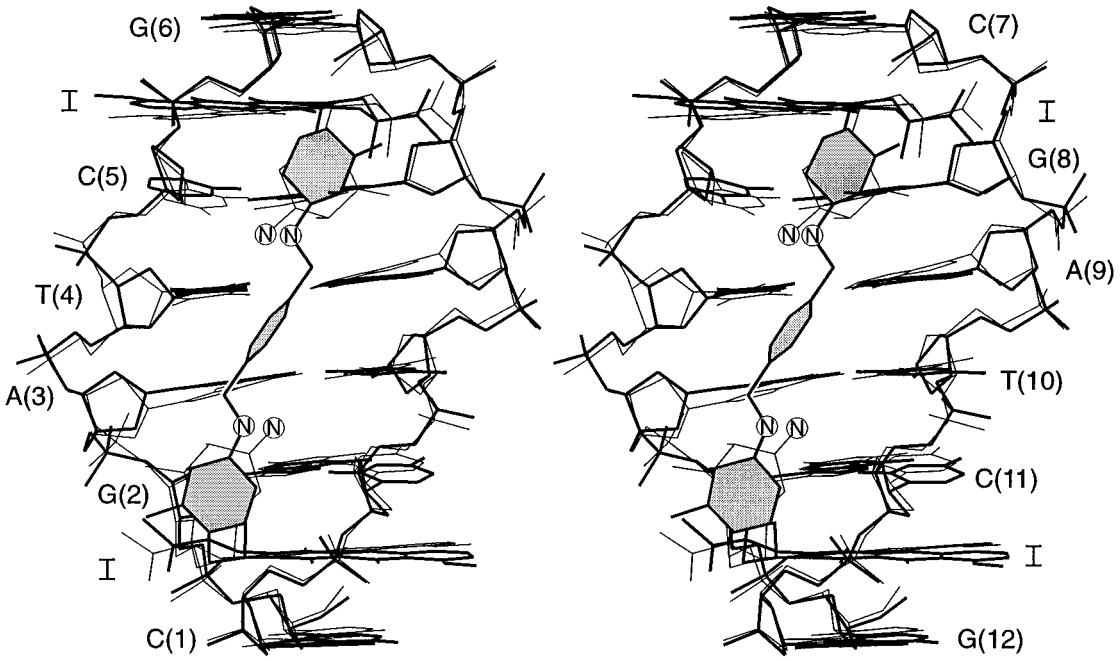

FIGURE 4: Stereoview of the WP631−[d(CGATCG)]$_2$ complex (thick lines) superimposed on the daunomycin$_2$−[d(CGATCG)]$_2$ complex (thin lines). The amino sugars and xylyl group of WP631 are shaded. The N3′ of WP631 and daunomycin are each labeled by an N. The residues are labeled, and each intercalative moiety is denoted by an I.

Table 2: Differences in Helical Parameters of WP631−[d(CGATCG)]$_2$ and Daunomycin$_2$−[d(CGATCG)]$_2$

	intra-base pair parameters		local inter−base parameters					
base pair	propeller twist (deg)	buckle (deg)	step	helical twist (deg)	roll (deg)	tilt (deg)	shift (Å)	slide (Å)
1-12	−0.6	−1.0	1−2	−1.1	0.2	0.6	−0.4	0.0
2-11	0.3	0.9	2−3	6.8	0.2	6.8	1.0	1.5
3-10	−10.0	6.1	3−4	−5.3	−4.0	−3.4	0.4	0.3
4-9	−10.0	−6.1	4−5	0.7	9.5	1.7	−0.4	1.0
5-8	0.3	−0.9	5−6	−0.9	−0.8	1.6	0.2	0.1
6-7	−0.6	−1.0						

greatest difference in interbase tilt is at the G(2)−A(3) step ($\Delta tilt_{2-3} = 6.8°$), while the greatest difference in roll is at the T(4)−C(5) step ($\Delta roll_{4-5} = 9.5°$). The central A-T base pairs show significant negative propeller twist in the WP631 complex but not in the daunomycin complex [Δpropeller $twist_{A(3)-T(10)} = -10°$]. Conversely, the central A-T base pairs show significant positive buckle in the daunomycin complex but not in the WP631 complex [$\Delta buckle_{A(3)-T(10)} = 6.1°$].

The long axes of the chromophores of both WP631 and daunomycin are oriented roughly perpendicular to those of the flanking base pairs. Hydrogen bonds from the 9-hydroxyl group of the daunomycin to the N2 and N3 of G(2) are conserved in the WP631 complex. Hydrogen bonding interactions can be observed in the ball and stick representation shown in Figure 5. It has been shown that the 9-hydroxyl group is essential for daunomycin activity (Plumbridge & Brown, 1979). Therefore, conservation of these hydrogen bonds is a critical benchmark of design success. In comparison with the chromophore of daunomycin, the chromophore of WP631 is rotated around a line roughly defined by the short axis of the chromophore. This rotation is consistent with slight strain in the linker.

The minor groove binding mode of the amino sugar is conserved. However, the location and interactions of the amino sugar within the minor groove are not. In the daunomycin complex, the 3′-amino nitrogen forms three hydrogen bonds with the DNA [to O2 of T(10), O2 of C(11), and O4′ of C(11)]. These interactions are lost in the WP631 complex, in which the 3′-amino group lacks hydrogen bonds with the DNA. Conservation of the hydrogen bonding interactions of the amino sugar was not a design goal; the extent of hydrogen bonding between DNA and the amino sugar is not related to activity. In many DNA−anthracycline complexes, the amino sugar forms hydrogen bonds with the DNA. However, the amino sugar of mono-intercalated 4′-epiadriamycin lacks hydrogen bonds to d(TCTACA) (Leonard et al., 1992), just as that of WP631 lacks hydrogen bonds to d(CGATCG).

The shift in the position of the amino sugar is accompanied by subtle changes in the conformation of the A ring (Δtorsion $< 6°$ for each angle; Table 3) and larger changes in torsion angles of the glycosidic linkage itself. These torsion angles are denoted by ω ($\Delta\omega = 15°$) and ψ ($\Delta\psi = -26°$) in Figure 6 and Table 3. In part as a consequence of these differences in torsion angles, the positions of the amino nitrogen of WP631 and daunomycin differ by 1.2 Å in the superimposed complex (Figure 4).

One surprising feature of the WP631 complex is a near absence of stabilizing van der Waals interactions between the amino sugar/linker and the minor groove of the DNA. A van der Waals interaction is defined here as a non-hydrogen bonding interatomic distance of less than 3.4 Å. By this definition, each intercalated chromophore forms 20 van der Waals contacts with the DNA. Only six atoms (three crystallographically independent atoms) of the linker and

Table 3: Selected Torsion Angles (Degrees) in Anthracycline Structures

	A ring	free daun[a]	TGT-daun[b]	TGA-daun[c]	TGT-4′epia[d]	CGT-ddaun[e]	CGA-daun[f]	CGA-WP631[g]	σ^h
α	C10−C19−C20−C7	−5	−11	10	−1	−1	−5	−5	3.4
β	C20−C19−C10−C9	15	27	−2	14	16	27	24	5.6
χ	C19−C10−C9−C8	−40	−44	−35	−42	−39	−57	−52	6.6
δ	C10−C9−C8−C7	58	55	66	63	53	66	63	4.7
ϵ	C9−C8−C7−C20	−48	−40	−56	−50	−34	−47	−44	5.4
ϕ	C8−C7−C20−C19	20	14	18	18	10	18	15	3.3
	glycosidic								
ω	C20−C7−O7−C1′	−114	−125	−115	−142	−150	−140	−125	12.3
ψ	C7−O7−C1′−C2′	167	137	127	159	167	137	163	13.0

[a] From the X-ray structure of free daunomycin (Neidle & Taylor, 1977). [b] From the X-ray structure of daunomycin bound to d(TGTACA) (Nunn et al., 1991). [c] From the X-ray structure of daunomycin bound to d(TGATCA) (Nunn et al., 1991). [d] From the X-ray structure of 4′-epiadriamycin bound to d(TGTACA) [PDB entry 1d54 (Leonard et al., 1992)]. [e] From the crystal structure of 11-deoxydaunomycin bound to d(CGTsACG) [PDB entry 1d14 (Williams et al., 1990)]. [f] From the low-temperature X-ray structure of the daunomycin bound to d(CGATCG) [PDB entry152d (Lipscomb et al., 1994)]. [g] This report (PDB entry 1agl). [h] $\sigma(\lambda) = [(1/n)\sum_{i=1}^{n}(|\lambda_i|-|\bar{\lambda}|)^2]^{1/2}$ is a measure of the variability of torsion angle λ, with $\bar{\lambda} = (\sum_i \lambda_i)/n$. λ_i is the value of λ in structure i, and n is 6, the number of structures. The structure of daunomycin−d(TGATCA) was not included.

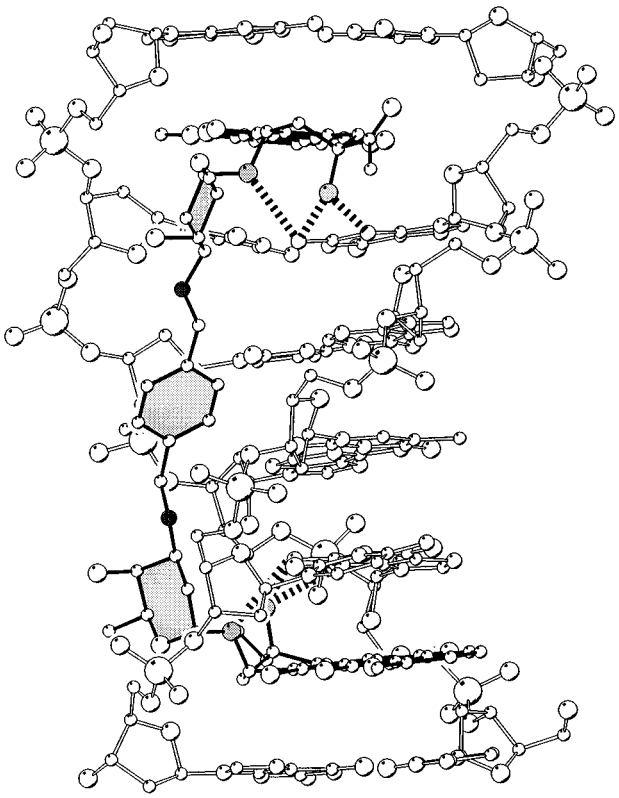

FIGURE 5: Ball and stick representation of the WP631−[d(CGATCG)]$_2$ complex. The atoms are sized by type with P > O > C > N. The bonds of WP631 are filled. The bonds of the DNA are open. The amino sugars and xylyl group and the N3′, O7, and O9 atoms of WP631 are shaded, with N3′ darker than O9 and O7. Hydrogen bonds between DNA and WP631 are represented by dashed lines.

amino sugar are in van der Waals contact with the DNA. The O5′ atoms of the amino sugar are each in van der Waals contact (3.34 Å) with the O4′ of a 5′-terminal guanosine [G(6) and G(12)]. These interactions, which are probably unfavorable, arise from the shift in position and orientation of the amino sugar in WP631 compared to that of daunomycin. The other contacts are in the center of the complex; the C9′a is in van der Waals distance of O2 of T(4) (3.22 Å), and C9′b is in van der Waals contact with O2 of T(10) (3.05 Å). The unfavorable oxygen−oxygen interaction and the deficit of stabilizing interactions of the linker/amino sugar with the DNA are further evidence that the linker is strained.

Fewer bound water molecules are observed in the WP631 complex than in the daunomycin complex. However,

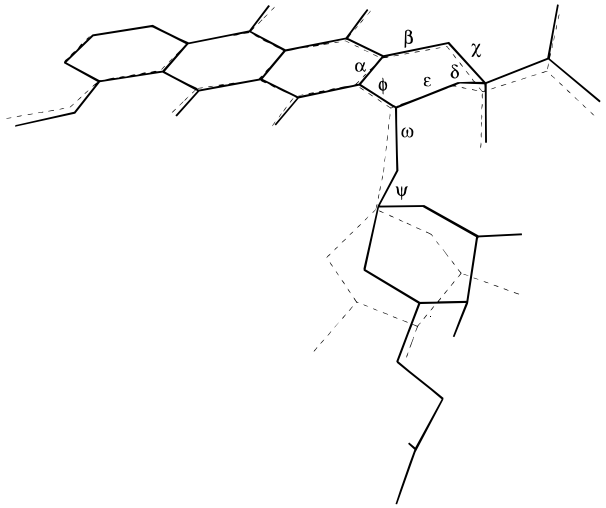

FIGURE 6: Comparison of conformations of WP631 and daunomycin. A view of the A ring and amino sugar moieties of WP631 (thick lines) and daunomycin (dashed lines) with the intercalative regions of the molecules superimposed.

differing numbers of observable water molecules are probably an artifact of the differing qualities of the crystals and the diffraction data (1.4 Å resolution for daunomycin and 2.2 Å for WP631). The crystals formed by daunomycin−d(CGATCG) are more highly ordered, resulting in more *observable* water molecules than crystals of WP631−d(CGATCG).

DISCUSSION

Design of DNA ligands by oligomerizing intercalators is evolving into an increasingly successful endeavor. TOTO and YOYO were successfully designed to act as highly sensitive DNA stains (Rye et al., 1992). Ditercalinium, designed as a chemotherapeutic agent, failed in the clinic but has been useful for study of mechanisms of DNA repair-induced cytotoxicity (Lambert et al., 1988) and DNA deformation (Peek et al., 1994; Williams & Gao, 1992). Bis-imidazoacridones, a new class of potent and highly selective antitumor agents, appear to be excellent candidates for clinical development (Cholody et al., 1995; Hernandez et al., 1995). These putative bis-intercalators are tetracyclic ring systems linked by a N^2-methyldiethylenetriamine or 3,3′-diamino-*N*-methyldipropylamine groups.

Structural considerations were paramount in the design of WP631 as a prospective chemotherapeutic agent. The three-

dimensional structure of two daunomycin molecules mono-intercalating in $[d(CGATCG)]_2$ was the template. The strategy succeeded; WP631 binds to DNA essentially as designed. The intercalation at terminal d(CpG) steps is conserved in the template mono-intercalator and designed bis-intercalator complexes. The hydrogen bonding interactions of the 9-hydroxyl group with N2 and N3 of G(2) (Figure 5) are conserved. Retention of these hydrogen bonding interactions is critical for success. The global location of the amino sugar in the minor groove is also conserved (Figures 3 and 4).

The WP631−DNA and daunomycin−DNA complexes provide the opportunity for detailed comparison of mono- and bis-intercalated complexes of the same chromophore. We observe that conversion from mono-intercalation to bis-intercalation alters the DNA conformation. Change is focused primarily in the center of the complex. DNA unwinding and other helical distortions propagate more efficiently to the center of the WP631 complex than to the center of the daunomycin complex.

The position and interactions of the amino sugar within the minor groove are not conserved in the bis-intercalated and mono-intercalated complexes. The malleabilities of these portions of the complexes are not surprising. The amino sugar is the most mobile portion of a daunomycin or adriamycin complex with DNA (Langlois d'Estaintot et al., 1992; Leonard et al., 1992; Lipscomb et al., 1994; Williams et al., 1990). The variability of the position of the amino sugar is consistent with a fairly flat potential well within the minor groove.

By modification of the linker, it may be possible to increase the affinity of WP631 for DNA. In template daunomycin-type complexes, two tightly bound water molecules (related by a 2-fold axis) are located within the minor groove. Tight binding of these water molecules is indicated by low thermal factors, a favorable geometry of interaction, and similar location and interactions in a variety of crystallographic environments. Each tightly bound water molecule in the template minor groove forms two hydrogen bonds to the floor of the groove and one hydrogen bond to the 3′-amino group of daunomycin. The linker of WP631 displaces these water molecules. Converting two mono-intercalated daunomycin molecules to one bis-intercalated WP631 molecule dehydrates hydrophilic functional groups of the DNA, forcing contact with a hydrophobic portion WP631. One might attenuate these unfavorable interactions by increasing the hydrophilic nature of the central portion of the linker, increasing the affinity of the bis-anthracycline for the DNA. In addition, it is conceivable that increasing the length of the linker could relieve strain and allow the linker and amino sugar to "relax" back to the floor of the minor groove, regaining van der Waals contacts.

As noted previously (Chaires et al., 1997), WP631 should bind to six base pair recognition sequences. Daunomycin binds preferentially to DNA triplets 5′-(A/T)CG and 5′-(A/T)GC, where (A/T) indicates either A or T (Chaires et al., 1990; Pullman, 1989). Therefore, WP631 is likely to bind preferentially to sequences such as 5′-CG(A/T)(A/T)CG and 5′-GC(A/T)(A/T)GC.

The three-dimensional structure of the WP631−DNA complex can help us to understand previously unexplained aspects of the energetics of the DNA binding reaction. The binding constant of a bis-intercalator is expected to be approximately the square of that of the monomer. However, the DNA binding constant for WP631 falls short of this theoretical limit. Its binding constant at 20 °C is 2.7×10^{11} M^{-1} compared to a value of 1.6×10^7 M^{-1} for daunomycin (Chaires et al., 1997). The lower than predicted binding affinity is consistent with differences in the DNA complexes of WP631 and daunomycin. In comparison with daunomycin, WP631 forms fewer hydrogen bonds with the DNA. The 3′-amino group of daunomycin forms hydrogen bonds with the floor of the minor groove that are absent in the WP631 complex. In addition, the daunosamine moiety of WP631 is lifted off the floor of the minor groove relative to its position in the daunomycin complex. Finally, several tightly bound water molecules are excluded from the minor groove in the WP631 complex. These three factors would result in an energetic penalty and can explain in part why the WP631 binding constant is not quite the square of that found for daunomycin. We emphasize, however, that the DNA binding of WP631 is ultratight and that its binding affinity for DNA approaches that observed for the binding of many regulatory proteins to their specific DNA sites. The structural data presented here can point to specific modifications that might be made in the next generation of bis-anthracyclines that can produce new compounds with even higher DNA binding affinities.

NOTE ADDED IN PROOF

An NMR structure of a complex of WP631 bound to $[d(ACGTACGT)]_2$ was described by Dr. Andrew H.-J. Wang at the annual meeting of the American Chemical Society in New Orleans, March 24−28, 1996. The features of the WP631−DNA complexes obtained by NMR and by X-ray crystallography are consistent, although there appear to be differences in the orientation of the xylene linker.

ACKNOWLEDGMENT

We thank Lori McFail-Isom, Tina Conti, and Rebecca Woo for helpful discussions.

REFERENCES

Boulad, F., & Kernan, N. A. (1993) *Cancer Invest. 11*, 534−553.

Chaires, J. B., Dattagupta, N., & Crothers, D. M. (1985) *Biochemistry 24*, 260−267.

Chaires, J. B., Herrera, J. E., & Waring, M. J. (1990) *Biochemistry 29*, 6145.

Chaires, J. B., Satyanarayana, S., Suh, D., Fokt, I., Przewloka, T., & Priebe, W. (1996) *Biochemistry 35*, 2047−2053.

Chaires, J. B., Leng, F., Przewloka, T., Fokt, I., Ling, Y. H., Perez-Soler, R., & Priebe, W. (1997) *J. Med. Chem. 40*, 261−266.

Cholody, W. M., Hernandez, L., Hassner, L., Scudiero, D. A., Djurickovic, D. B., & Michejda, C. J. (1995) *J. Med. Chem. 38*, 3043−3052.

Hernandez, L., Cholody, W. M., Hudson, E. A., Resau, J. H., Pauly, G., & Michejda, C. J. (1995) *Cancer Res. 55*, 2338−2345.

Krishnamoorthy, C. R., Yen, S.-F., Smith, J. C., Lown, J. W., & Wilson, W. D. (1986) *Biochemistry 25*, 5933−5940.

Lambert, B., Segal-Bendirdjian, E., Roques, B. P., & Le Pecq, J.-B. (1988) in *DNA Repair Mechanisms and Their Biological Implications in Mammaliam Cells* (Lambert, M. W., & Laval, J., Eds.) pp 639−652, Plenum Press, New York.

Langlois d'Estaintot, B., Gallois, B., Brown, T., & Hunter, W. N. (1992) *Nucleic Acids Res. 20*, 3561−3566.

Leonard, G. A., Brown, T., & Hunter, W. N. (1992) *Eur. J. Biochem. 204*, 69−74.

Lipscomb, L. A., Peek, M. E., Zhou, F. X., Bertrand, J. A., VanDerveer, D., & Williams, L. D. (1994) *Biochemistry 33*, 3649−3659.
Neidle, S., & Taylor, G. (1977) *Biochim. Biophys. Acta 479*, 450−459.
Nunn, C. M., Van Meervelt, L., Zhang, S. D., Moore, M. H., & Kennard, O. (1991) *J. Mol. Biol. 222*, 167−177.
Peek, M. E., Lipscomb, L. A., Bertrand, J. A., Gao, Q., Roques, B. P., Garbay-Jaureguiberry, C., & Williams, L. D. (1994) *Biochemistry 33*, 3794−3800.
Plumbridge, T. W., & Brown, J. R. (1979) *Biochim. Biophys. Acta 563*, 181−192.
Pullman, P. (1989) in *Advances in Drug Research* (Testa, B., Ed.) Vol. 18, pp 1−113, Academic Press, Boston.
Remeta, D. P., Mudd, C. P., Berger, R. L., & Breslauer, K. J. (1991) *Biochemistry 30*, 9799−9809.
Rizzo, V., Sacchi, N., & Menozzi, M. (1989) *Biochemistry 28*, 274−282.
Ross, D. D. (1991) *Curr. Opin. Oncol. 3*, 21−29.
Rye, H. S., Yue, S., Wemmer, D. E., Quesada, M. A., Haugland, R. P., Mathies, R. A., & Glazer, A. N. (1992) *Nucleic Acids Res. 20*, 2803−2812.
Valentini, L., Nicolella, V., Vannini, E., Menozzi, M., Penco, S., & Arcamone, F. (1985) *Il Farmaco 40*, 377−390.
Williams, L. D., & Gao, Q. (1992) *Biochemistry 31*, 4315−4324.
Williams, L. D., Egli, M., Ughetto, G., van der Marel, G. A., van Boom, J. H., Quigley, G. J., Wang, A. H.-J., Rich, A., & Frederick, C. A. (1990) *J. Mol. Biol. 215*, 313−320.

BI9705218